

Safety of ropeway drives against slipping

Monitoring of rope slipping using a camera

G. Oplatka and M. Roth

1. Problem

A chair lift with fixed grips had problems with adhesion of the haul rope on the drive sheave. In order to monitor the slip of haul rope it was decided to fix a camera and a floodlight on the drive sheave to rotate synchronously with it (Fig. 1 und 2). The loading of chairs by bales of straw corresponded approximately the maximum loading allowed. Rope axial slip and rope twist could be derived from the visual material obtained.

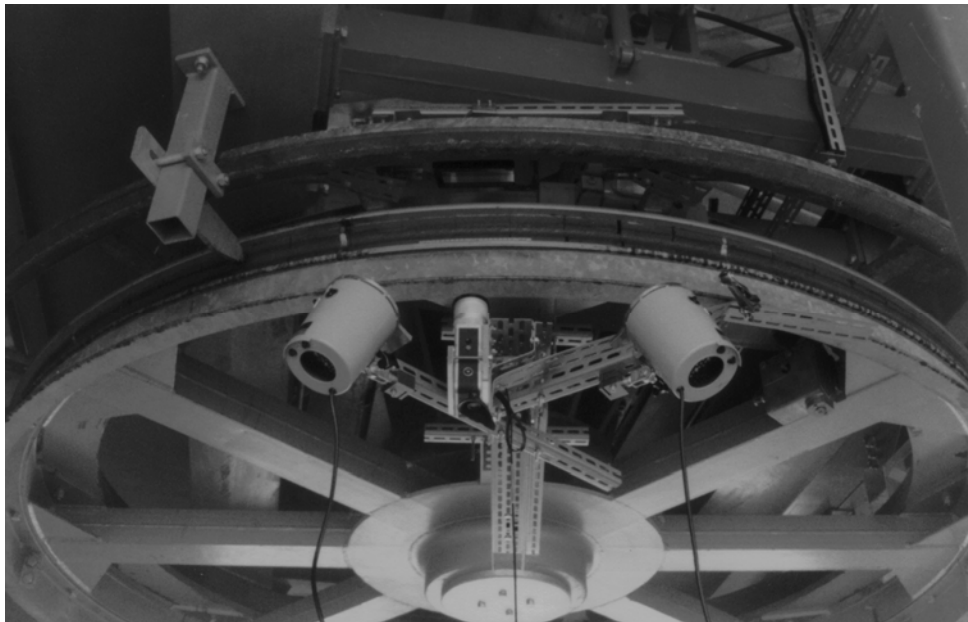


Fig. 1: Test equipment: A film camera and two floodlights mounted on the drive sheave to rotate synchronously with it. The camera takes pictures of specific points on the rope, that enable the calculation of the relative speed between drive sheave and rope.

Prof.Dr.Dr.h.c.G.Oplatka, Eur Ing Dipl.Ing. M. Roth, Institute of Lightweight Structures and Ropeways, Swiss Federal Institute of Technology, ETH-Zentrum LEO
CH-8092 Zürich, Tel: ++41.1 633 25 10, Fax: ++41.1 633 11 10,
e-mail: oplatka@ils.mavt.ethz.ch; roth@ils.mavt.ethz.ch

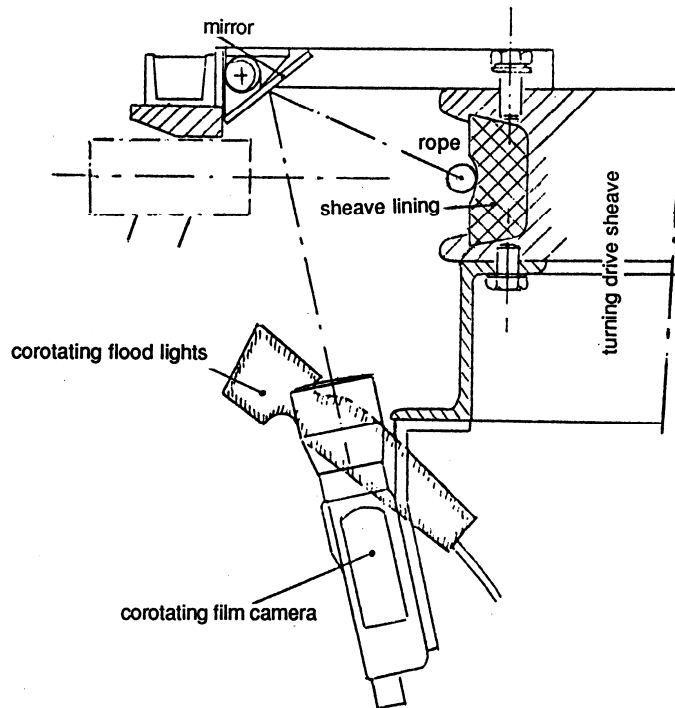


Fig. 2: Layout of the film equipment

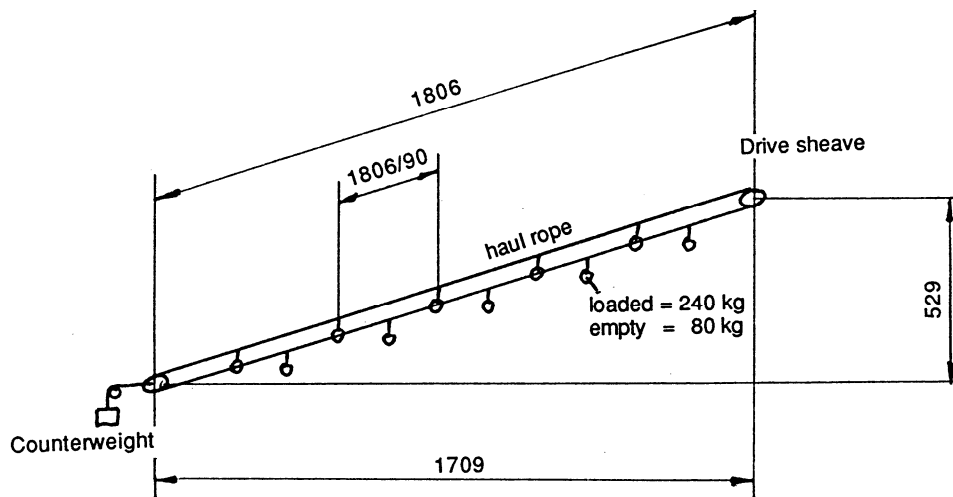


Fig. 3: Schematic arrangement of the investigated chair lift

- maximum rope tension: appr. 125 kN
- drive sheave: 3010 mm DIA, rubber lining
- surrounding angle 180°
- haul rope: 32 mm DIA, Lang's lay, Seale 6x19+FC

2. Theory

2.1. General

During operation of a ropeway a helical slip motion of the rope occurs on the drive sheave. It proceeds approximately in the direction of the strands. The slip motion's axial component is approximately proportional to the tensile force difference ΔS between the coming up and going away branch sections of the rope. The axially directed slip speed (also called: creep speed) v_c is also proportional to tensile force difference ΔS .

2.2. Creep speed v_c

For the calculation of the **theoretical** creep speed the following formula has been used:

$$v_c^{theor} = \frac{\Delta S}{E \cdot A} \cdot v \quad [mm/s] \quad (\text{eq. 1})$$

with: ΔS Difference of rope forces calculated according to the loading of chairs as well as from the electrical power input of the drive motor
 E modulus of elasticity of the rope = 10^5 N/mm^2
 A metallic cross section of the rope = 386 mm^2
 v rope speed (evaluated from the number of recorded images of film; maximum: 2.0 m/s)

The **measured** creep speed was obtained by using single images of the film *) for the quantities in the expression:

$$v_c^{meas} = \frac{\Delta x_2 - \Delta x_1}{\Delta t} \quad (\text{Equation 2})$$

whereby: Δx_1 indicates axial displacement by position „1“ of fixed point.
 Δx_2 indicates axial displacement by position „2“ of fixed point.
 Δt time interval for corresponding turn angle of drive sheave.

*) The rope was observed at the singled out point („fixed point“) from the moment of coming up onto the sheave (0°) to the moment of going away from the sheave (180°).

3. Evaluation of the films

Four films have been made and evaluated:

- **Film No. 1:** loaded uphill travel / empty downhill travel
- **Film No. 2:** loaded uphill / empty downhill (the same loading case as in Film No. 1)
- **Film No. 3:** loaded downhill / empty uphill: continuous electrical braking
- **Film No. 4:** loaded downhill / empty uphill: including start phase

Images of the „fixed point“ on the rope were recorded on each film from the time the point entered the sheave until it, having travelled 180° around the sheave. Both the axial creep component (Δx) and the corresponding components y and Δy of torsion were determined from the images. The value of rope torsion ($\Delta\Phi$) was computed. Fig. 4 shows the relationship between y , Δy and $\Delta\Phi$. Figures 6, 7 and 8 show plots of these values as a function of the position of the fixed point on the sheave.

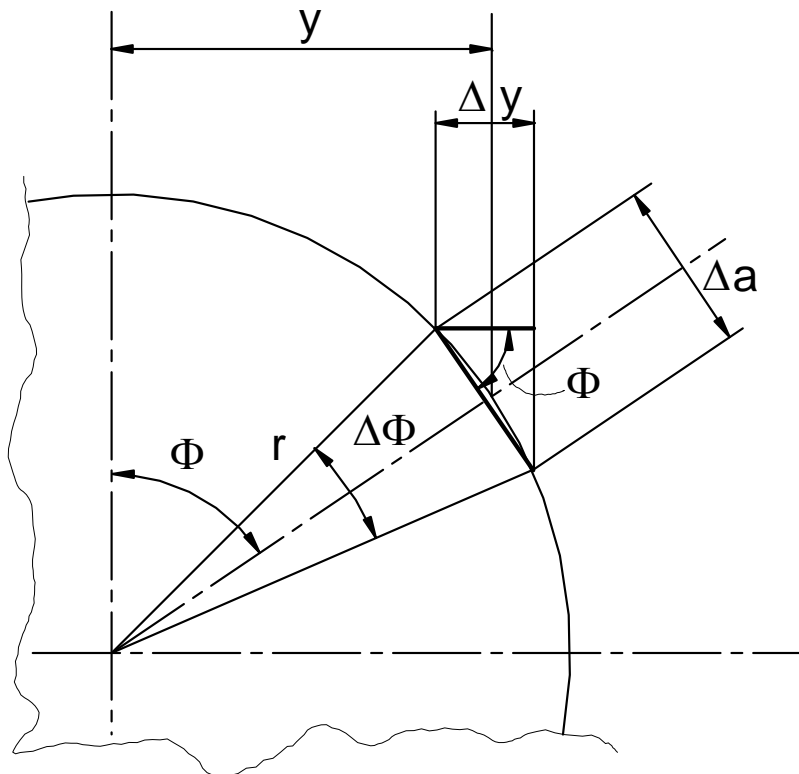


Fig. 4: Conversion of y and Δy into the angle of rope torsion $\Delta\Phi$

$$\Delta\Phi = 2 \cdot \arcsin \frac{\Delta y}{2 \cdot \sqrt{r^2 - y^2}}$$

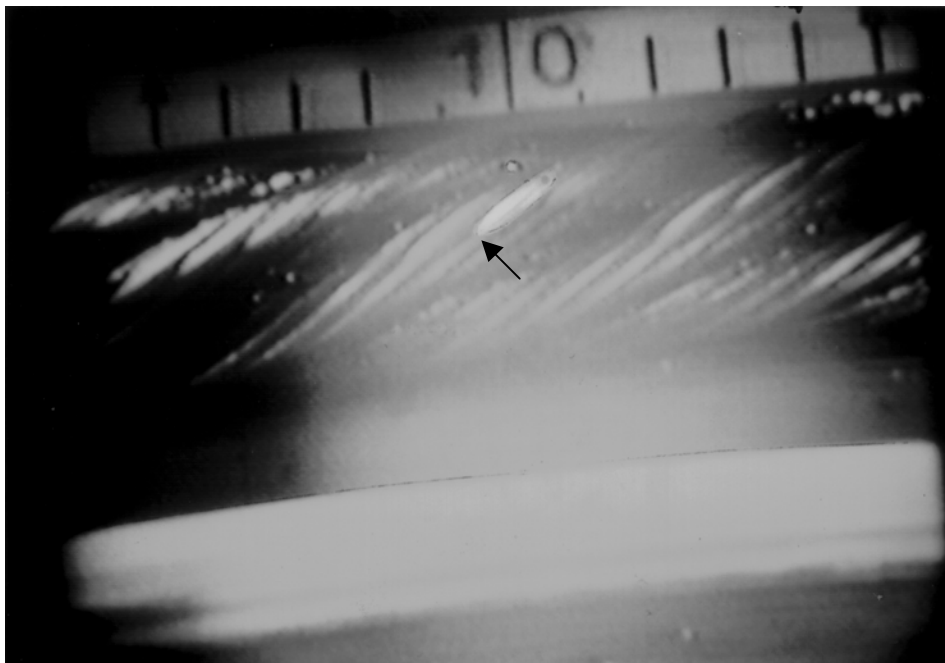


Fig. 5: Creep movement sheave lining.
Upper image: fixed point coming up onto sheave (0°).
Lower image: fixed point going away from sheave (180°).
The axial displacement of fixed point: $\Delta x = 3.5$ mm, the torsional angle of displacement obtained by conversion: $\Delta\Phi = 5.5^\circ$.

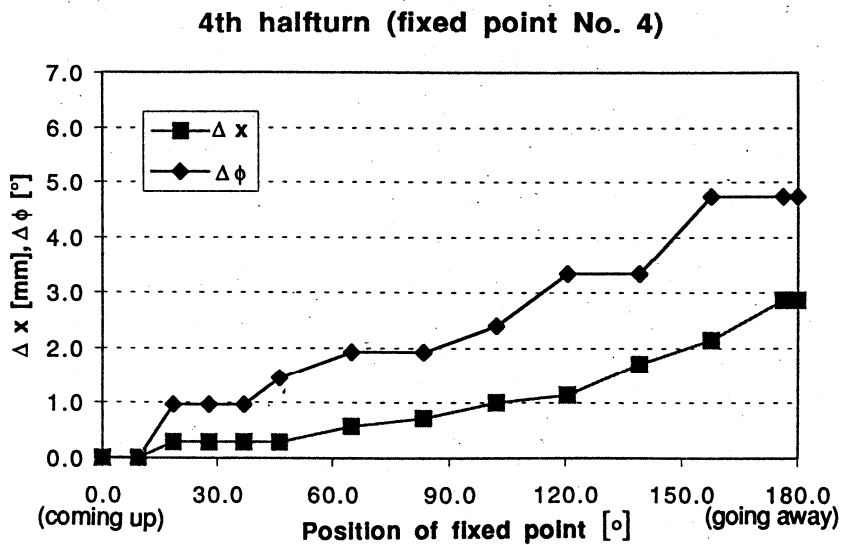
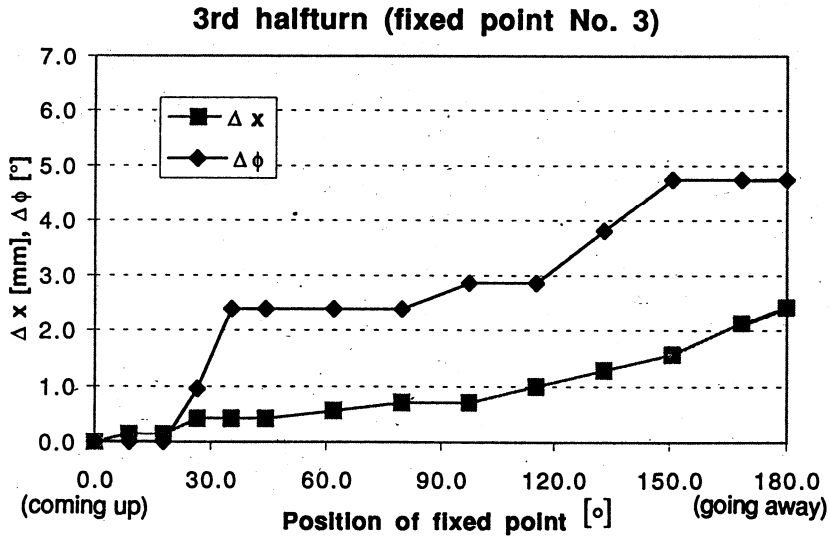


Fig. 6: Film No. 1: loaded uphill travel / empty downhill travel

Horizontal axis: positions of the fixed point. The scale starts at the point coming onto the sheave (0°) and finishes where it leaves it (180°). This corresponds to a halfturn of the sheave.

Vertical axis: axial displacement Δx and torsional angle $\Delta\Phi$ of the fixed point.

The very similar course of such plots is displayed in Fig. 7 (3rd and 4th halfturn of the drive sheave).

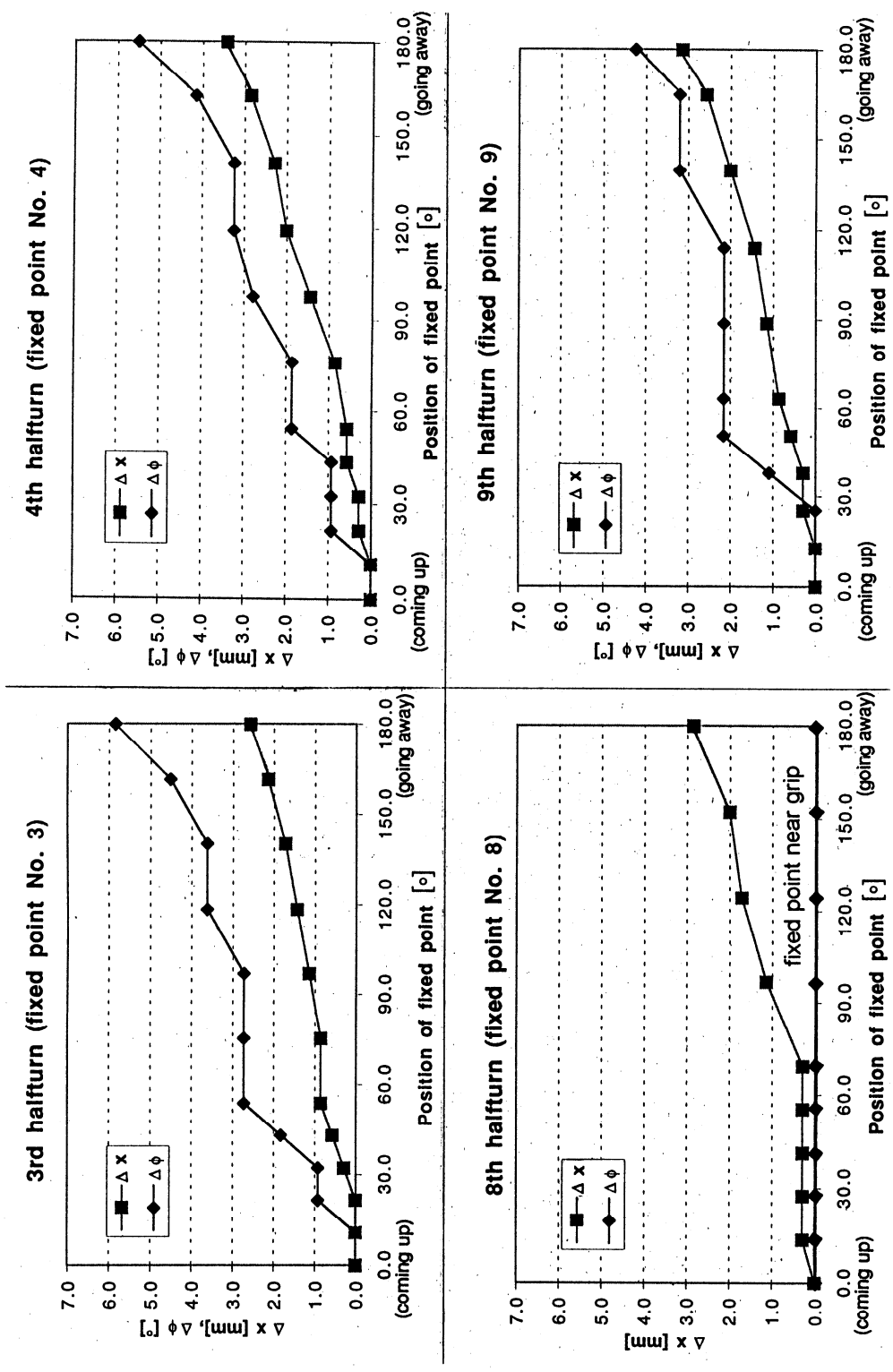


Fig. 7: Film No. 4: loaded uphill travel / empty downhill travel
 Upper image: fixed point coming up onto sheave (0°)
 Lower image: fixed point going away from sheave (180°)

Note the curve for the 8th half-turn with marked point near the grip: while the axial displacement Δx is similar to that in other curves, the value of rope torsion $\Delta \Phi$ stays zero, showing that there was no twist in the rope.

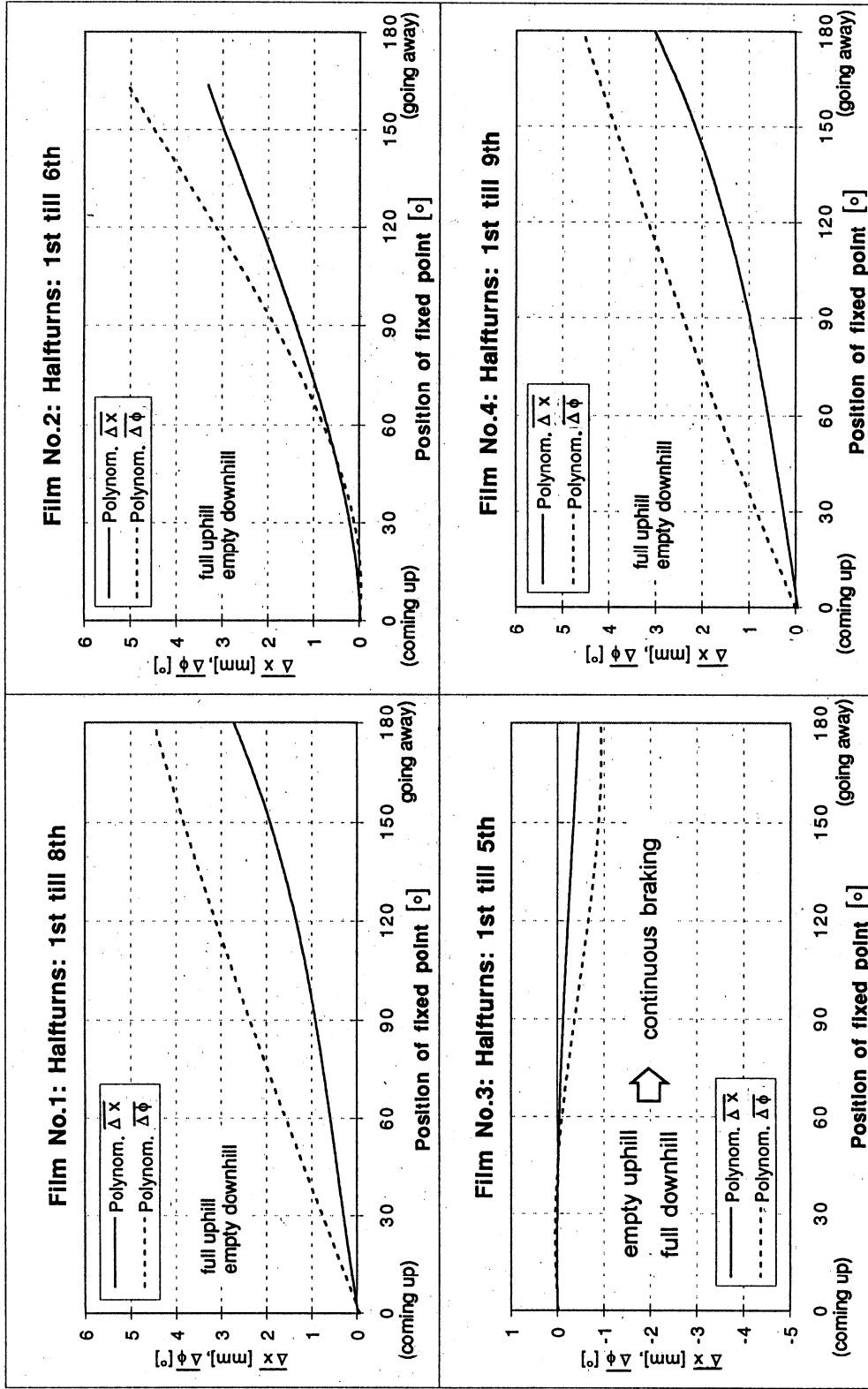


Fig. 8: The mean value of the axial slip Δx and the mean value of the torsional angle $\Delta \phi$ computed as mean value of several measurements (compare Fig. 6 and 7) according to polynomials of third order. The evaluations according to polynomials of second order and fourth order give very similar results.

4. Measurement results

4.1. Measurement accuracy

An estimation of measuring error was carried out with the comparison measurement by the third halfturn from film No. 1. It was based on the possible reading accuracy of $\pm 0.2\text{mm}$ on the monitor. Thus results an error of $\pm 0.3\text{mm}$ for axial displacement. The error for the angle is $\pm 1.0^\circ$. Due to this great error of the angles, the $\Delta\Phi$ graphs at smaller values are to be interpreted with caution.

4.2. Mean creep speed v_c [mm/s]

Film / loading	Theoretically calculated from -		Measured - using polynomial for Δx (Figs. 6,7, 9 and eq. 2)
	tensile forces in both rope branches [kN]	measured electric input power to drive [kW]	
#1: loaded uphill	1.44	2.09	1.34
#3: loaded downhill	1.07	1.36	0.80
#4: loaded uphill	2.25	1.91	1.66

5. Conclusions

Based on evaluation and calculation of theoretical axial slip it was concluded that the observed slip is based on elastic elongation of the rope and **not** that an actual „slipping through“ on the drive sheave occurred in case of this chair lift.

6. Evaluation of the method of measurement and suggestions for improvement

Points for possible improvement have been noted during the measurement and in the evaluation of images. These will be discussed in this section.

a) By this method the exact position of grip by the single turns is **often** unknown. Thereby no statement can be given about the influence of the grips on the creep speed and on the torsional angle.

b) It was difficult to adjust the camera so as to have the rope, the sheave and the centimeter-scale all in sharp focus. In future a camera with a lens having a better depth of focus may have to be used. Fig. 9 indicates the problem.

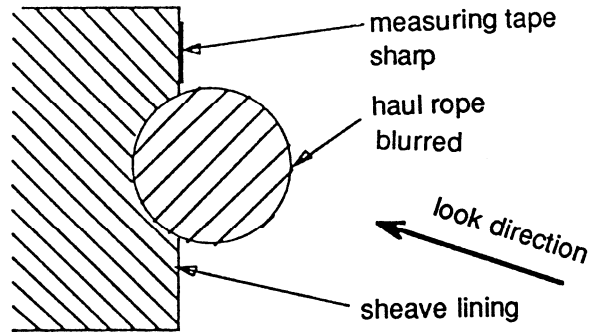


Fig. 9: The depth of focus

c) The measured points were mostly light reflections, because no other fix points of the rope could be followed. The problem by these light reflections is that not all of them are stationary clear on the rope. That means it first must be checked whether such points change positions on the rope surface. If they do not, the light spot can be applied as „fixed point“ for measurements.

d) In the case the fixed point on the rope is marked, the marking must be small enough to identify the point accurately. Color drops of some 0.5 mm diameter should make the mark well readable while providing sufficient accuracy for locating the point.

e) To fix another tape measure along the rope as a marker resulted in blurred and inaccurate images because the tape did not lay nicely on the rope.

f) The images of the film may be evaluated with a film-viewer or a microfilm viewer. The former has the advantage that the film may be run through quickly and the rope be monitored for movement. If particular sections are to be viewed at larger magnification, this may be done with the aid of the microfilm viewer.

g) A single source of light was used in the experiments. This resulted images with too high contrast. If the rope is to be examined in more detail it should be illuminated from two or more sources mounted on the sheave.

h) Both depth of focus and the problem of marking and detecting the point of interest on the rope may be improved by using a digital camera with possibility of direct image processing on a computer.

7. Bibliography

- [1] Czitary, E. Seilschwebbahnen, pages 404-415. Springer Verlag, Wien 1962
- [2] Oplatka, G. Seilbahnen I (lecture notes), pages 7.71 /1- 6. ETH Zürich, 1998
- [3] Hajduk, J. Der Reibungschluss zwischen Drahtseil und gummigefütterter Antriebsscheibe. Internationale Seilbahnrundschau, Heft Mai (Sonderdruck)/ 1959
- [4] Kollros, W. The Relationship Between Torque, Tensile Force and Twist in Ropes. Internationale Seilbahn-Rundschau, Heft 2 / 1974
- [5] Oplatka, G./Canale, R. Zur Treibfähigkeit von Treibscheiben - Entwicklung eines Schlupfmessgerätes. Kongress „Neue Technologien im Materialfluss und in der Fördertechnik“, TU Karlsruhe, 10.-12. April 1985